Separation and Purification Technology 305 (2023) 122523

Contents lists available at ScienceDirect

Separation and Purification Technology

journal homepage: www.elsevier.com/locate/seppur

A novel, green, cost-effective and fluidizable SiO_2-decorated calcium-based adsorbent recovered from eggshell waste for the CO_2 capture process

Mehri Imani [a], Maryam Tahmasebpoor [a,*], Pedro Enrique Sánchez-Jiménez [b,*], Jose Manuel Valverde [c], Virginia Moreno [b]

[a] Faculty of Chemical & Petroleum Engineering, University of Tabriz, Tabriz PO Box 51666-16471, Iran
[b] Instituto de Ciencia de Materiales de Sevilla, C. S. I. C.-Universidad de Sevilla, C. Américo Vespucio no 49, 41092 Sevilla, Spain
[c] Faculty of Physics, University of Seville, Avenida Reina Mercedes s/n, 41012 Sevilla, Spain

ARTICLE INFO

Keywords:
CO_2 capture
Calcium looping
Eggshell
Sol-gel
Hydration
Fluidization

ABSTRACT

The reduction, storage, and reuse of greenhouse gas carbon dioxide (CO_2) is a crucial concern in modern society. Bio-waste adsorbents have recently aroused the investigator's attention as auspicious materials for CO_2 capture. However, the adsorption capacity decaying and poor fluidizability during carbonation/calcination cycles of all natural adsorbents used in the calcium-looping process (CaL) are important challenges. The current study explores the performance of a novel SiO_2-decorated calcium-based adsorbent recovered from eggshell waste in terms of both CO_2 capture capacity and fluidity. Two preparation methods of hydration and sol–gel were used to obtain Ca-based adsorbents with different pore configurations and volumes. Modification of the adsorbents was applied by dry physically mixing with different weight percentages of hydrophobic SiO_2 nanoparticles (NPs), in order to maintain stability and fluidity. The adsorbent prepared by the sol–gel method exhibited a fluffier structure with smaller grain sizes and higher porosity than that of prepared by the hydration method, leading to a 6.9 % increase in conversion at the end of the 20th cycle. Also, with the optimal amount of SiO_2 nanoparticles, i.e. 7.5 wt%, the amount of CaO conversion obtained by sol–gel derived adsorbent was 27.59 % higher than that by pristine eggshell at the end of the 20th carbonation/calcination cycles. The fluidizability tests showed that the highest bed expansion ratio (2.29) was achieved for sol–gel derived adsorbent in the presence of 7.5 wt% silica nanoparticles which was considerably higher than the amount of 1.8 and 1.6 belonged to sol–gel derived adsorbent and pristine eggshell without silica at the gas velocity of ≈ 6.5 cm/s, respectively. The high adsorption capacity and proper fluidity of this novel and green calcium-based adsorbent promise its wide application.

1. Introduction

Global warming which is the long-term heating of Earth's climate system and occurred due to human activities (primarily fossil fuel burning) leads to the increases in heat-trapping greenhouse gas levels in Earth's atmosphere [1]. By reducing emissions of CO_2 as the main greenhouse gas, we can reduce the risks of harmful climate catastrophes such as large-scale flooding and droughts that deprives larger populations of their homes, livelihoods, or even lives [2]. Taking into account these dangerous effects of CO_2 releasing, finding powerful means to reduce its emission is receiving increased attention, recently.

The calcium looping process (CaL) or the regenerative calcium cycle (RCC) is a carbon capture technology, in which calcium is reversibly reacted between its carbonate form ($CaCO_3$) and its oxide form (CaO) to separate CO_2 from other gases released from power plants [3]. The CaL process can be studied at a lab-scale fluidized bed reactor or thermo gravimetric analyzer (TGA) system, both of which have two main stages, including calcination and carbonation, which happens reversely [4]. During carbonation, adsorbent particles react with the CO_2 in the flue gas at a temperature of about 650 °C to form $CaCO_3$, thereby reducing the CO_2 concentration in the flue gas to an allowed level for emission to the atmosphere. The carbonated particles are then circulated into the calciner and heated up to 800–950 °C under a highly concentrated CO_2 stream to produce gaseous carbon dioxide and solid calcium oxide via thermal decomposition, so they are regenerated for a new cycle and fed back to the carbonator [5]. In the carbonation stage, a fast initial reaction rate is suddenly followed by a slow reaction rate. The ratio of moles of CO_2 reacted in the rapid reaction step to its stoichiometric value in the

* Corresponding authors.
E-mail addresses: tahmasebpoor@tabrizu.ac.ir (M. Tahmasebpoor), pedro.enrique@icmse.csic.es (P. Enrique Sánchez-Jiménez).

https://doi.org/10.1016/j.seppur.2022.122523
Received 31 August 2022; Received in revised form 23 October 2022; Accepted 27 October 2022
Available online 1 November 2022

complete conversion of CaO to $CaCO_3$ is defined as the adsorption carrying capacity [6].

It is worth mentioning that minerals were first explored in the CaL process but since then the use of wastes is also gaining acceptance. Using cheap and easily-accessible biological waste as CO_2 absorbent has the advantage of continuous injection due to the deactivation phenomenon. Moreover, management and disposal of the large amount of biological waste produced in restaurants, industries and homes has become one of the important environmental concerns [7]. In this regard, Sun et al [8] applied prewashing treatment to lime mud and considered its performance for removing of CO_2. They reported the beneficial effect of prewashing in leading to the higher CO_2 capture capacity and improving its microstructure in comparison with the lime mud through the carbonation process. In another research, Pizarro et al [9] investigated the acetic acid modified steel slag CO_2 capturing performance. They concluded that the residence time and the calciner temperature reduced in high CO_2 partial pressure at 900 °C. Similarly Ma et al [10] used carbide slag as a base material for preparing the CO_2 adsorbent with high alumina cement and by-product of biodiesel. After applying the real operational conditions including high temperature and high CO_2 concentration, they discussed that highest CO_2 capture capacity of about 0.27 g/g was obtained for the adsorbent contained 90 wt% CaO after 30 carbonation/calcination cycles which was 1.7 times higher than that for carbide slag. The major $CaCO_3$ containing bio-waste which can be a proper option for the industrial CaL process is eggshell [11–13]. There are a few challenges that need to be overcome to facilitate the commercial implementation of CaL technology. One of them is related to the progressive deactivation of the CaO. Since $CaCO_3$ has a larger molar volume in comparison to CaO, the carbonated layer growing effectively blocks the pores, and finally the carbonation is restricted by gas diffusion [14]. Also, the high temperatures attained during calcination, about 900–950 °C, result in substantial particle agglomeration and sintering [15,16]. Further increase in temperature along with longer calcination times can affect the intensity of sintering, whereas carbonation time has minimal effect on particle sintering [17]. The reduction in reactive surface area and a corresponding decrease in capture capacity are the main disadvantages of sintering whose negative effects need to be reduced by applying proper methods.

On the other hand, since the industrial-scale CaL process is performed in the fluidized bed reactors, the adsorbent's fluidization behavior and the effective gas–solid contact are also very important in evaluating the overall efficiency of the process [18]. Therefore, applying modification methods that not only increase the adsorption capacity but also improve the adsorbent fluidity, are essential. Recently, many studies have been carried out to improve the performance of calcium-based adsorbents in the cyclic process by incorporating inert materials. For example, Jing et al [19] incorporated Al to CaO by sol–gel method in order to obtain $CaO/Ca_3Al_2O_6$ sorbents. Initial pretreating was performed at 800 °C for 10 min to remove CO_2 and H_2O adsorbed from the air and then carbonation was carried out at 500 °C for 30 min under 10 %CO_2/90 %N_2 atmosphere. It was reported that with the mass ratio of 8:2 for CaO: Al_2O_3, a superior CO_2 sorption ratio of 51.92 % was obtained which was 5 times higher than that of the pure CaO sorbent. In line with previous research, Azimi et al [20] developed CaO-based sorbent mixed with Al_2O_3 using the sol–gel method and found that stability and cyclic CO_2 capture performance were improved due to the formation of $Ca_9Al_6O_{18}$. Similarly, Koirala et al [21] studied the role of adding various metals such as Al, W, Ce to Zr/Ca adsorbents. The best performance was obtained by Al due to the $Ca12Al14O33$ formation, which was a more stable component. In another work, Li et al [22] doped CaO-based adsorbent with $KMnO_4$ at different concentrations ranging from 0.5 to 0.8 wt%. They reported that the long-term performance of $CaCO_3$ was enhanced so that after 100 cycles the conversion of $KMnO_4$-doped adsorbent was increased to 0.35 while it was just 0.16 for pure $CaCO_3$ in the same conditions. Furthermore, Heidari et al [23] proposed synthetic CaO-based sorbents modified by mono-metallic (Zr, Al, Ce), bi-metallic (Zr/Ce, Zr/Al, Al/Ce), and tri-metallic (Zr/Al/Ce) inert oxides. Among the synthesized sorbents, Ca/Zr/Al/Ce with 17.8 % deactivation after 50 cycles, was introduced as the most promising adsorbent in terms of capture capacity. Valverde et al [24] considered the role of adding nanosilica physically to $Ca(OH)_2$ powder as a base sorbent for CO_2 capturing during the CaL process in a TGA at conditions close to the real CaL looping process. They concluded that adding nanosilica in a specific molar ratio enhanced the rate of fast carbonation and residual capture capacity. There were also other studies emphasized on the positive role of silica nanoparticles in improving fluidity. Amjadi et al [25], used hydrophobic silica nanoparticles to enhance the $Ca(OH)_2$ fluidization quality and successfully reported that 20 wt% of SiO_2 nanoparticles had 2.24 times higher bed expansion ratio compared to as received $Ca(OH)_2$ at gas velocity of 0.05 m/s. As well, Azimi et al [20] founded that synthesized Ca-based adsorbent by sol gel method, had very homogeneous fluidization behavior after adding $>$ 15 wt% hydrophobic SiO_2 nanoparticles. Also, in our most recent published article [26] in which acid modified eggshell particles were mixed physically with hydrophobic silica nanoparticles, it was revealed that using SiO_2 nanoparticles not only improve the fluidity but also increase the adsorption capacity. Therefore, it seems that adding various weight percentages of silica nanoparticles may affect the eggshell particles adsorption performance.

As far as we know; no studies on simultaneous increases of CO_2 capture capacity and fluidity of low-cost eggshell-derived calcium-based adsorbents have been conducted yet. So, in this work we concentrate on dry mixing of SiO_2 nanoparticles, as an additive, at various weight percentages, with eggshell-derived calcium-based adsorbent, searching for a balanced improvement of cyclability and fluidizability. In order to investigate the effect of the preparation method on the performance of adsorbents recovered from eggshells, two methods were used: hydration and sol–gel. Leading to the formation of the same form of final product i.e. $Ca(OH)_2$, simplicity, low-cost and having the possibility of comparison the results could be mentioned as the main reasons for selecting these two preparation methods. The best-performing adsorbents in several carbonation/calcination cycles were selected and tested in a fluidized bed in terms of their fluidity performance. To characterize the phase composition, morphology, and capturing capacity, X-ray diffraction (XRD), Scanning electron microscopy (SEM), Brunauer-Emmett-Teller (BET), and TGA analysis were conducted. Particle size distribution (PSD) analysis was also used to determine the synthesized particle sizes. Finally, to consider the fluidization behavior of adsorbents, two parameters including bed expansion ratio and pressure drop were measured for pristine eggshell and modified adsorbents.

2. Experimental section

2.1. Materials

2.1.1. Chemicals

The initial eggshell waste was collected from local restaurants in Tabriz. After washing the eggshell particles with deionized water, taking their inner tissues away, and drying them at 60 °C in the oven, the pristine eggshell was obtained. Hydrophobic SiO_2 nanoparticles (Aerosil® 974) with high SiO_2 content ($>$99.8 %), BET surface area of 150–190 m^2/g, and also a mean particle size distribution of 94 nm were purchased from Evonik. Hydrochloric acid (37 %), NaOH, and $CaCl_2$ purchased from Sigma Aldrich were used to synthesize the adsorbents with the sol–gel method.

2.1.2. Preparation of adsorbent by hydration method

As a first step, the eggshells were washed with deionized water to remove all possible pollution. Then, their inner tissues were removed and after drying at 60 °C in the oven, the clean eggshells were crushed in a porcelain mortar and pest. To have more uniform powder the electric mill was used and particles were passed through a 325-mesh screen (dp

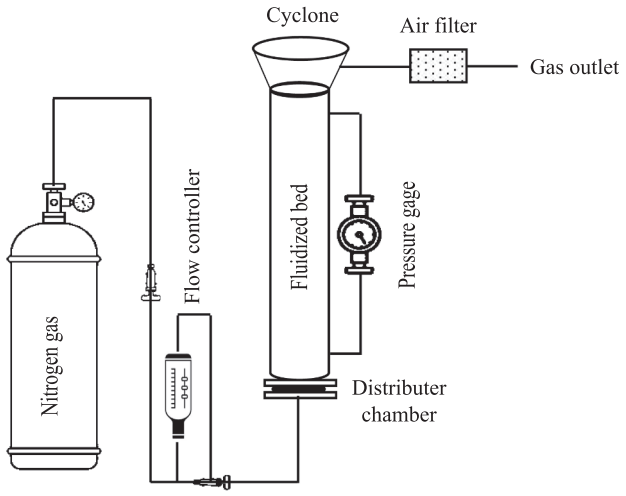

Fig. 1. The schematic of fluidization system.

< 45 μm). Calcium hydroxide was achieved by hydration method during which the eggshell-derived calcium carbonate powder was refluxed in distilled water at 60 °C for 6 hr, according to the below equation:

$$CaCO_3 + H_2O \rightarrow Ca(OH)_2 + CO_2 \quad (1)$$

After drying at 60 °C in the oven, the $Ca(OH)_2$ white powders were turned into the sample named hydrated eggshell in the following [27–29].

2.1.3. Preparation of adsorbent by sol–gel method

To prepare the eggshell-derived adsorbent by sol–gel method, the eggshell particles were first washed, the tissue removed, crushed, and sieved with a 325-mesh, in a similar way to the hydration method. Then, 12.5 mg of eggshell powder was solved in 250 mL of 1 M HCl solution to produce a sol as a result of the following reaction:

$$CaCO_3 + 2\,HCl \rightarrow CaCl_2 + H_2O + CO_2 \quad (2)$$

Then, 250 mL of 1 M NaOH solution was dropwise added to the sol containing $CaCl_2$, after which the following reaction occurred:

$$CaCl_2 + 2\,NaOH \rightarrow Ca(OH)_2 + 2\,NaCl \quad (3)$$

The prepared solution was aged for one night at room temperature to obtain a gel. Then, it was filtrated and washed with distilled water. Finally, the gel was dried at 60 °C for 24 hr. The final product will be named sol–gel derived adsorbent hereafter [30].

2.1.4. Dry mixing of SiO_2 nanoparticles

Hydrated eggshell and sol–gel derived adsorbent were physically mixed with SiO_2 nanoparticles to improve their performance in terms of adsorption capacity and fluidization behavior. For this purpose, aerosol® 974 nanoparticles were first sieved using a 150 μm sieve to remove the possible agglomerates and then added to the above-mentioned samples by hand dry mixing method for 30 min. Adding various weight percentages of SiO_2 nanoparticles including 2.5, 5, 7.5, and 10 wt % were tested in this study.

2.2. Fluidization tests

Fluidization tests were performed in a fluidized bed consisting of an 80 cm glass column with an inner diameter of 2.6 cm at 25 °C and atmospheric pressure. The schematic of the fluidized bed is presented in Fig. 1. Pure nitrogen gas (>99.98 %) was introduced to the bed through the high porous plate distributor. A cyclone and an air filter were installed to have a clean gas in the output of the bed. The fluidization behavior of the particles was interpreted by two parameters named bed expansion ratio (H/H_0) and pressure drop (Δp). H_0 was attributed to the initial bed height when no nitrogen gas entered the bed and H was the bed attitude at the specific gas velocity. A monometer (pressure gage Wika) was installed between the top of the column and distributer to measure the pressure drop (Δp) of the bed during the fluidization of particles. Both parameters were measured against different gas velocities controlled by a gas flow meter. All the experiments were repeated 3 times with 5 min time intervals between two tests in order to achieve the highest accuracy as well as stable condition.

2.3. Characterization techniques

2.3.1. Structural characterizations

SEM was used to evaluate the surface structure and morphology of as-prepared adsorbents before and after the adsorption process. All morphological analyses were performed by applying a HITACHI S4800 SEM-FEG microscope: cold cathode field emission gun with voltage from 0.5 to 30 kV, resolution of 1 nm at 15 kV. Equipped with a Bruker-X Flash-4010 EDX detector with a resolution of 133 eV (at the MnKα line), and a detector with sample holder to work in transmission mode (STEM-in- SEM). All the samples were coated with a thin layer of gold by Emitech K550 Telstar sputter-coating machine at 30 mA for 30 s. PSD analysis was measured using a Mastersizer 2000 (Malvern). All samples were sonicated in isopropanol solution using Elma ultrasonic LC 130H; for 30 min to improve homogeneity and reduce the probable agglomerate sizes. Additionally, BET analysis was performed with Tristar II 3020 apparatus where N_2 isotherms were measured at 77 K. The crystalline phase of as-prepared samples before carbonation/calcination cycles was determined by (XRD) using a Rigaku Miniflex diffractometer over an angular range of $10^\circ < 2\Theta < 70^\circ$, at 40 kV and 15 mA. By analyzing of XRD results, the crystallite size of adsorbents was calculated using Scherrer's equation [31]:

$$D = \frac{K^*\lambda}{\beta \cos\theta} \quad (4)$$

Where D is the average crystallite size in nm, K is the constant shape factor, λ is the wavelength of X-ray, β is the width at half the maximum values in radians and θ is the Bragg angle.

2.3.2. Capture capacity measurements

Twenty carbonation/calcination cycles were conducted in a thermo gravimetric analyzer TG5500 in order to measure the CO_2 capture capacity of pristine eggshell, hydrated eggshell and sol–gel derived adsorbent. The weight of the sample loaded into the TGA was 11 mg which was initially heated up to 800 °C under pure nitrogen with a heating rate of 300 °C/min and then kept for 5 min, to ensure full conversion to CaO. The carbonation stage was then performed at 650 °C for 5 min under 15 vol% of CO_2 and 85 vol% of N_2 atmosphere. After complete carbonation, the gas was switched to N_2 and the temperature increased to 800 °C at 300 °C/min and maintained isothermally for 5 min to start the calcination step. These cycles were repeated 20 times for all the samples. The performance of the prepared adsorbents in terms of the mass of CO_2 adsorbed and CaO molar conversion were evaluated by calculating of samples' weight change. The CaO molar conversion could be reported by the following equation [32]:

$$\text{CaO molar conversion}\,(\%) = \frac{w_t - w_i}{w_i} * \frac{1}{0.786} \quad (5)$$

Where w_t is the weight of sample at time t, w_i is the initial weight of the sample, and 0.786 is the theoretical mass uptake capacity of CO_2 by CaO (44 g CO_2/56 g CaO).

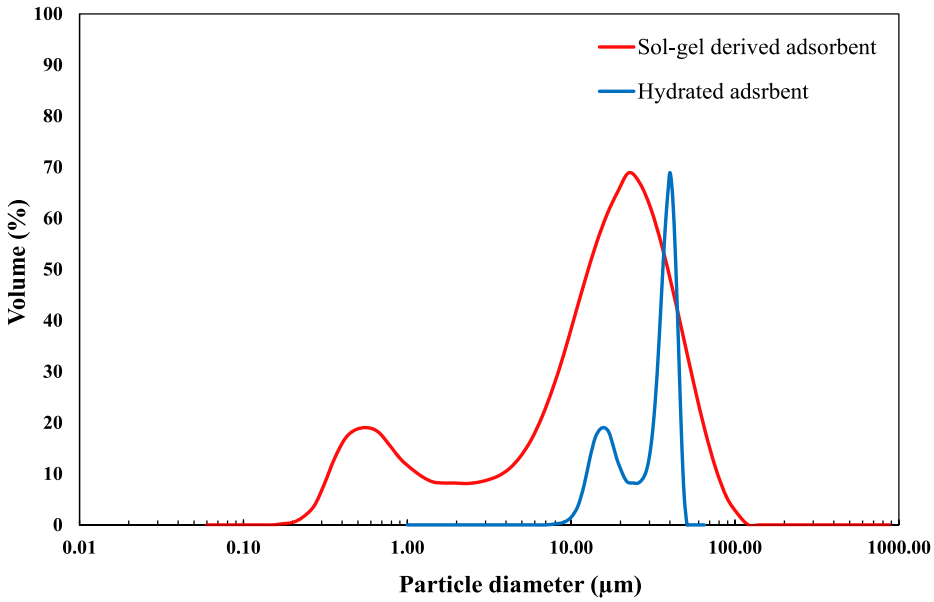

Fig. 2. Particle size distribution of hydrated eggshell and sol–gel derived adsorbent.

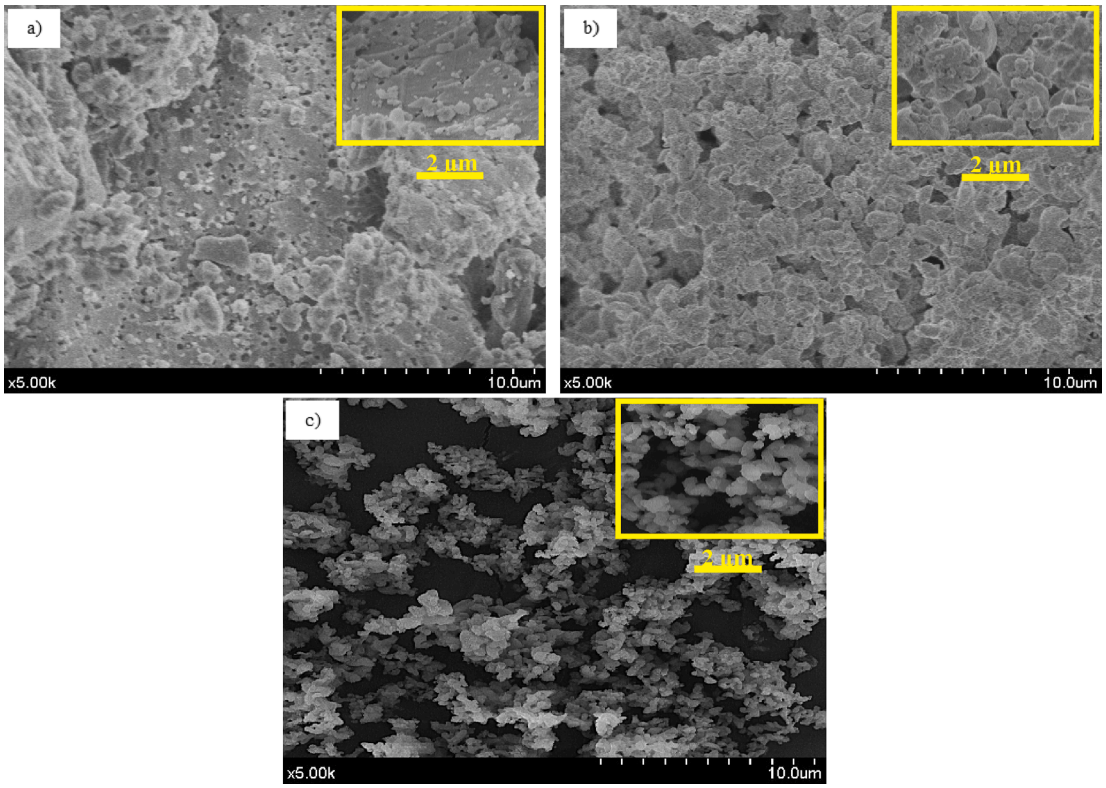

Fig. 3. SEM images of (a) pristine eggshell, (b) hydrated eggshell and (c) sol–gel derived adsorbent.

3. Results and discussion

3.1. Characterization of the adsorbents

The results of particle size distribution analysis for hydrated eggshell and sol–gel derived adsorbent, are shown in Fig. 2. According to this figure, hydrated eggshell exhibits a bimodal PSD with maxima in the mesopore region (17 and 41 μm). Similar bimodal results appear for sol–gel derived adsorbents with the difference of the peaks emerging at very low sizes including 0.5 and 20 μm. Also, the hydrated eggshell had a much narrower size distribution than particles synthesized via the sol–gel method. The hydrated eggshell has essentially no particles in the dp < 10 μm size range, while sol–gel derived adsorbent volume percentage is noticeably great for small sizes ($0.13\ \mu m < dp < 10\ \mu m$). As reported in the literature [33,34], particle size distribution plays an important role in CO_2 capture capacity, since by increasing of particle size, pore plugging could limit the surface area and decrease the CaO conversion, which will be investigated in the following sections.

The effect of preparation methods including hydration and sol–gel on the structure of eggshell-derived adsorbents was investigated by SEM. As

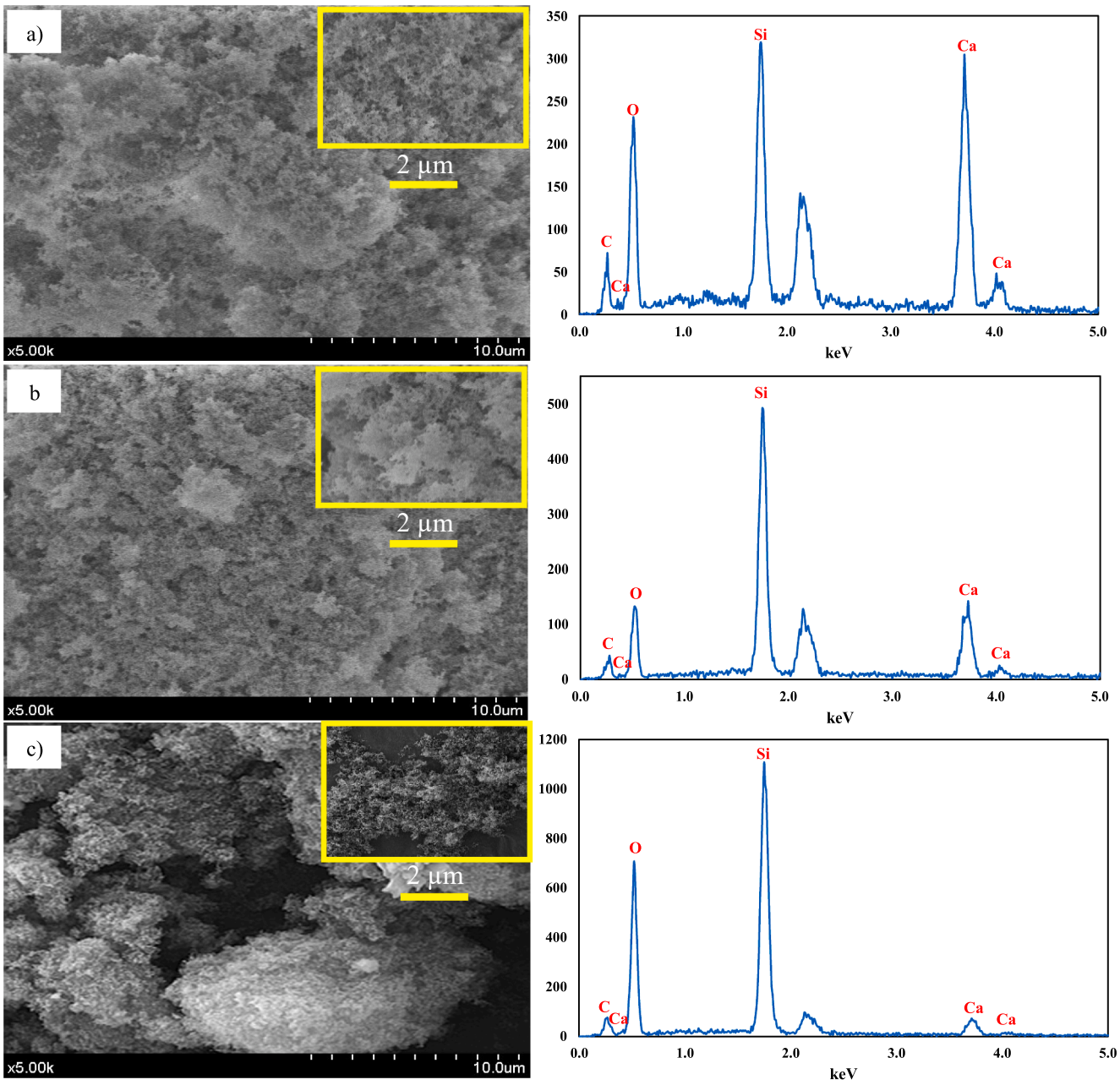

Fig. 4. SEM images and elemental analysis of (a) pristine eggshell, (b) hydrated eggshell and (c) sol–gel derived adsorbent, mixed with 7.5 wt% silica NPs.

seen in Fig. 3, pristine eggshell is mostly in the form of sharp-edged crystals with little porosity and a smooth surface. Also, the morphology differences seen in Fig. 3b and c confirm that both preparation methods lead to a more porous structure as compared with pristine eggshell particles, which look more compact and solid-like (Fig. 3a). Furthermore, by comparing Fig. 3b and c, it was evident that the sol–gel method made a fluffier structure with smaller grain sizes and more open porosity as compared to the hydration method. This morphology changes refer to the chemical reaction that occurred during the synthesizing of $CaCO_3$ particles by sol–gel method in which the hydrochloric acid encouraged the straining of the crystalline matrix and the formation of additional vacancies [35].

To address the covering quality of host and guest particles on each other, SEM analysis was again used on the pristine and hydrated eggshell and also on sol–gel derived adsorbent while all were mixed with silica nanoparticles. In this regard, samples mixed with 7.5 wt% hydrophobic silica nanoparticles were examined and SEM micrographs as well as elemental analysis are presented in Fig. 4. According to the previous study carried out by Amjadi et al [37], in which the $Ca(OH)_2$ adsorbents were mixed with 150 and 600 nm silica NPs, the elemental mapping analysis confirmed that surface of the aggregates of $Ca(OH)_2$ particles have become uniformly covered with SiO_2 nanoparticles. Similiarly, as can be seen the aggregates of particles in all three mentioned samples have become uniformly covered with SiO_2 nanoparticles, hence homogeneous mixing was obtained. It may be discussed that strong attraction electrostatic forces were established at the contact points between the hydrophobic SiO_2 nanoparticles and the samples particles due to contact charging [36,37]. The presence of silica nanoparticles also affected the morphologies by reducing the crystallite sizes as a result of their dispersion in the adsorbent's lattice. For instance, based on equation (4), the crystallite size was calculated as 28 nm for sol–gel derived adsorbent containing 7.5 wt% SiO_2, while the corresponding amount for its silica-free sample was 42 nm. Also, by comparing Figs. 3 and 4, it could be noted that the smaller particle size and the more porous structure also

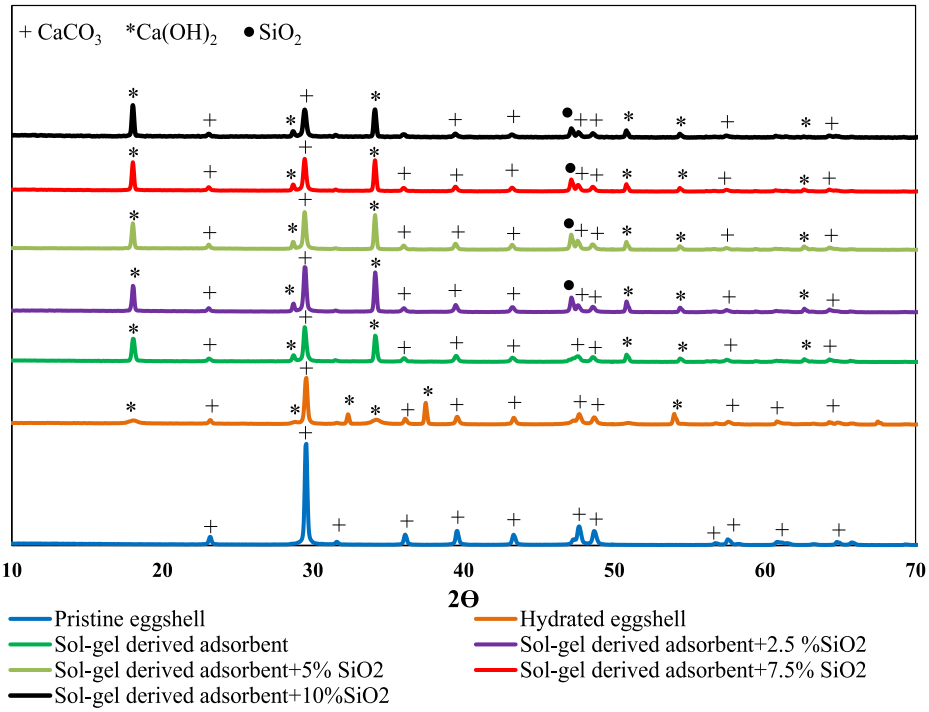

Fig. 5. XRD patterns of pristine eggshell, hydrated eggshell and sol–gel derived adsorbent mixed with various wt% of silica NPs.

Table 1
Specification of pristine eggshell, hydrated eggshell and sol–gel derived adsorbent before and after mixing with 7.5 wt% silica NPs.

Samples	Surface area, BET (m^2/g)	BJH Desorption cumulative volume of pores (cm^3/g)	Total pore volume (cm^3/g)
Pristine eggshell	6.13	0.017480	0.011784
Hydrated eggshell	6.15	0.018641	0.013725
Sol-gel derived adsorbent	7.14	0.029884	0.019218
Pristine eggshell + 7.5 % SiO_2	13.00	0.037138	0.027564
Hydrated eggshell + 7.5 % SiO_2	13.75	0.038526	0.029314
Sol-gel derived adsorbent + 7.5 % SiO_2	14.87	0.049783	0.032688

appeared in the silica-containing samples, i.e., the small particles led to high porosity. All these differences in the adsorbents' structure probably could affect their cyclic adsorption performances, because normally CO_2 diffuses more easily through the porous and fluffy structure than a dense layer to reach the unreacted adsorption sites.

XRD analysis was used to study the hydrated eggshell, sol–gel derived adsorbent, and also those modified with different weight percentages of silica nanoparticles. The corresponding patterns are presented in Fig. 5. The main reflection peaks in pristine eggshells which correspond to calcium carbonate, with calcite structure. It is clear that both hydration and sol–gel methods result in the formation of calcium hydroxide, although calcium carbonate is still dominant. The XRD patterns of silica-containing sol–gel derived adsorbents indicated the presence of SiO_2, $CaCO_3$ and $Ca(OH)_2$.

Physical properties such as surface area and porosity mainly affect the gas adsorption performance of calcium based adsorbents in calcium looping process [38]. Therefore, the textural specifications of pristine eggshells, hydrated eggshells and sol–gel derived adsorbents along with those mixed with 7.5 wt% silica nanoparticles are presented in Table.1.

According to the results, preparation methods of hydration and sol–gel increased the BET surface area of adsorbents to 6.15 and 7.14 m^2/g, respectively, while the corresponding amount for pristine eggshell was 6.13 m^2/g. Also, applying the sol–gel method resulted in a quite larger BET surface area compared to the hydration method. It should be mentioned that the small difference of BET surface area values relies on the all samples' similarities in terms of micro- and *meso*-porosity [39], and the main difference is attributed to the more open porosity (macropores) of sol–gel derived adsorbent compared to the hydrated and pristine eggshells (clearly confirmed by SEM pictures of Fig. 3). A surprising result was also obtained from BET analysis demonstrating that adding silica nanoparticles could improve the surface area of all samples, in a way that the rate of incensement was about 2 times or even more. The corresponding amount of Barret- Joyner- Halenda (BJH) desorption cumulative volume of pores was also reported in Table 1, confirming the positive effect of the sol–gel method as well as adding silica nanoparticles. So that, the sol–gel method caused a 70.96 % increase in the volume of pores, while the amount reported for hydration method showed only 6.64 % improvement compared to pristine eggshell. Sol-gel derived adsorbent + 7.5 % SiO_2 presented the highest BJH desorption cumulative volume of pores (0.049783 cm^3/g). To clarify the effect of silica nanoparticles, the BJH desorption (dV/dD) pore volume distribution and N_2 physisorption isotherms for pristine eggshell and sol–gel derived adsorbent after dry mixing with 7.5 wt% of silica nanoparticles was displayed in Fig. 6 (the corresponding result was also provided for pure pristine eggshell for better comparison). As shown in Fig. 6a, the pore size distribution of the three mentioned adsorbents had a dominant peak at a pore size between 3 and 4 nm, which is in good agreement with the results reported in [40]. This was an envisaged outcome because the preparation method i.e. hand-dry mixing method for silica nanoparticle addition didn't change the pore distribution [41]. Likewise, the sol–gel derived adsorbent maintained the largest number of pores smaller than 10 nm, after mixing with silica nanoparticles. The above-mentioned results could promise the positive effect of silica nanoparticles as well as the sol–gel preparation method on the capture capacity of introduced adsorbent during CaL. Additionally, the similar N_2 physisorption isotherms of pristine eggshell and sol–gel

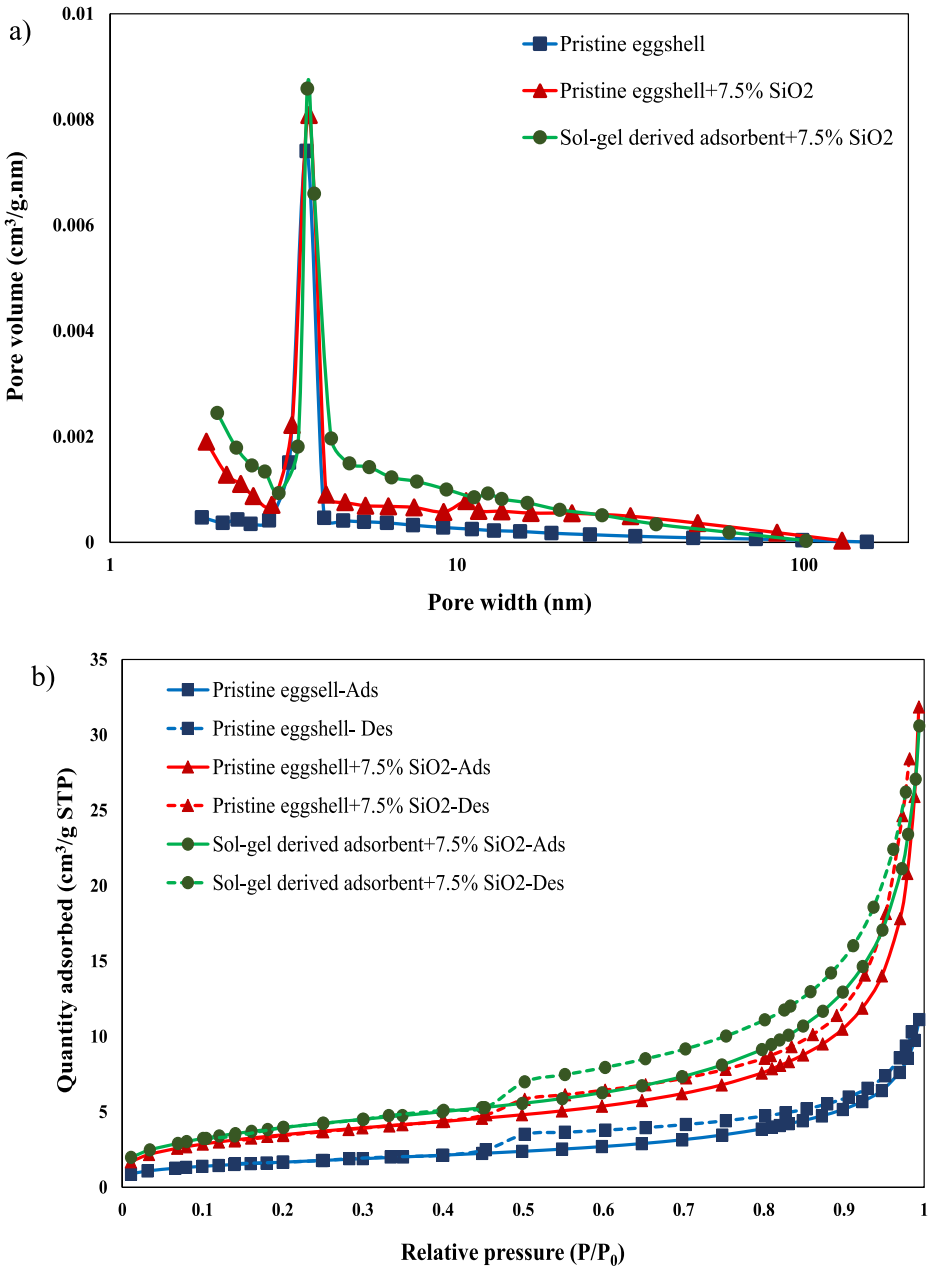

Fig. 6. a) BJH desorption (dV/dD) pore volume distribution and b) N_2 physisorption isotherm for pristine eggshell, pristine eggshell + 7.5 wt% silica NPs and sol–gel derived adsorbent + 7.5 wt% silica NPs.

derived adsorbent mixed with 7.5 wt% of SiO_2, (presented in Fig. 6b) could be related to type II mode based on Brunauer-Deming-Deming-Teller (BDDT) adsorption isotherm classification [42], normally indicating a nonporous or macroporous structure. Obviously, sol–gel derived adsorbent contained 7.5 wt% silica nanoparticles had higher adsorption than the other samples. In two P/P_0 ranges including 0.00 to 0.03 and 0.75 to 0.80 a sharp steep increase in N_2 adsorption was seen. Also, according to International Union of Pure and Applied Chemistry (IUPAC) hysteresis loop classification [43] the hysteresis loop type of H3 caused by capillary condensation of N_2 in mesopores along with the aggregates of plate-like particles lead to slit-shaped pores [44].

3.2. Sorption capacity

3.2.1. Effect of preparation method

Weight loss profiles of pristine eggshell, hydrated eggshell, and sol–gel derived adsorbent along with those mixed with 7.5 wt% silica nanoparticles are illustrated in Fig. 7, where $\Delta m/m_0$ is defined as weight loss per initial weight of the sample and calculated from TGA data. Once the adsorbent was settled down in TGA, the temperature was first increased to 800 °C at the rate of 300 °C/min in the N_2 atmosphere. According to Fig. 7 which is ascribed to the weight loss at the beginning of the process, by increasing the temperature two weight loss steps could be recognized. First, for all samples, the dehydration process occurred during preheating at about 100 °C and led to the adsorbent with a mixture of CaO and silica nanoparticles (in the case of silica NPs contained samples). During the first weight loss, the pristine eggshell, hydrated eggshell, and the silica-containing pristine eggshell experienced fewer weight decaying than sol–gel derived adsorbents (with or without silica nanoparticles). This phenomenon can be explained by the sample's structural differences recognized by XRD; the pristine eggshell which totally consisted of $CaCO_3$ and hydrated eggshell with a few $Ca(OH)_2$

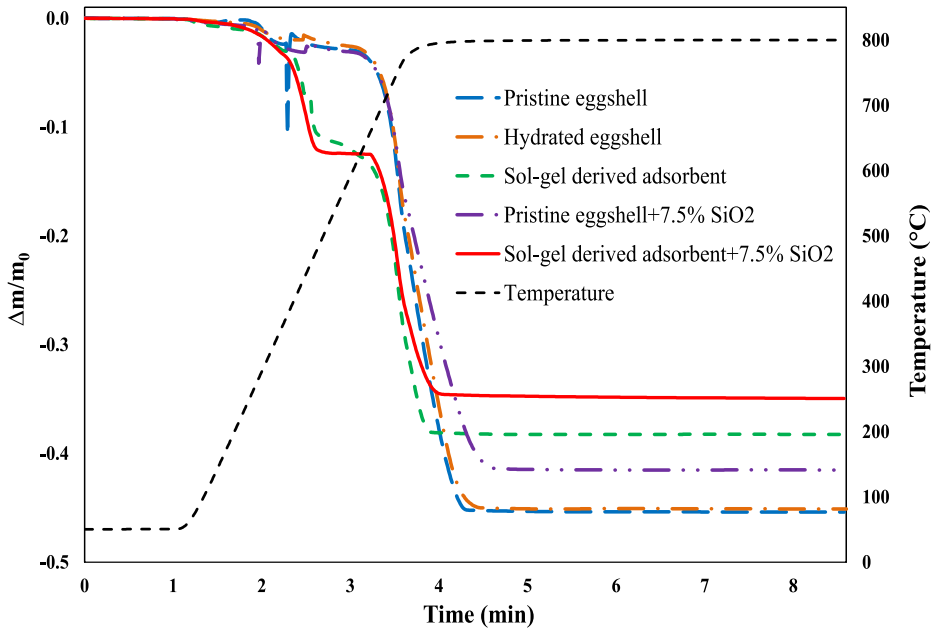

Fig. 7. Weight losing patterns of different adsorbents as a function of temperature and time during the pre-heating under N_2 atmosphere.

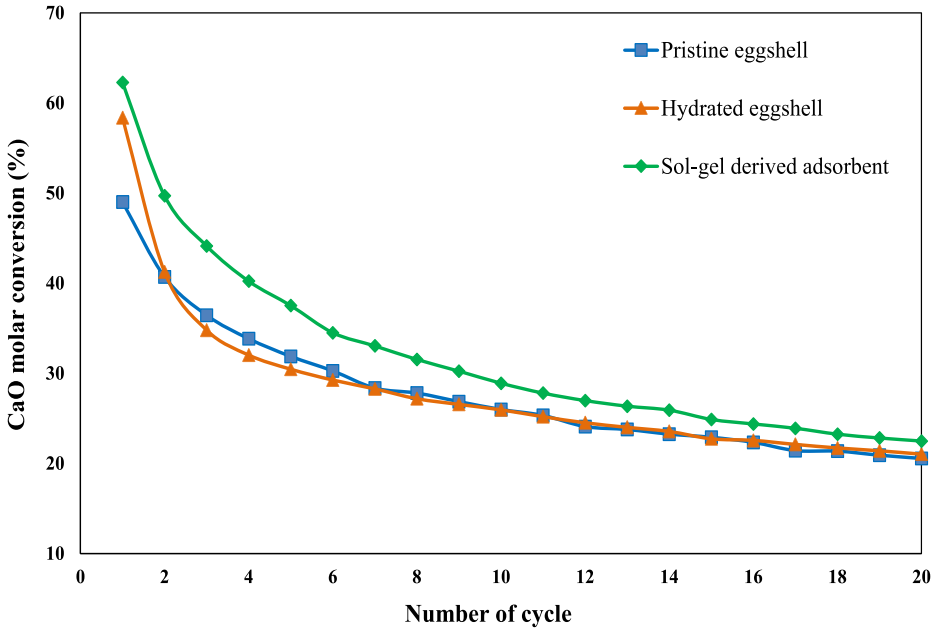

Fig. 8. CaO molar conversion of pristine eggshell, hydrated eggshell and sol–gel derived adsorbent.

content, was subjected to less dehydration compared to the sol–gel derived adsorbent with high calcium hydroxide portion. After preheating the second weight loss ascribed to CaO calcination was observed. The lower value of $\Delta m/m_0$ detected for sol–gel-derived adsorbent was due to the lower CO_2 enclosed in its interior compared to pristine and hydrated eggshells which could be imputed to the higher calcium hydroxide appearing during its synthesizing process. Additionally, by comparing the samples with and without silica nanoparticles, it was evident that the weight loss per initial weight of samples was decreased for silica-containing samples because silica nanoparticles with zero CO_2 content occupied some of the adsorbent pores. Also, it is worth mentioning that the second weight loss for pristine eggshell and hydrated eggshell occurred at 650 °C, while the sol–gel method decreased the weight loss temperature to 460 °C as well as the time, which was reduced to 2.6 min for sol–gel derived adsorbent compared to 3.23 min for both pristine and hydrated eggshell.

Fig. 8 compares the CaO molar conversion for pristine eggshell, hydrated eggshell and sol–gel derived adsorbent during 20 cycles under calcium looping conditions. First, it is clear that in all samples the amount of captured CO_2 decreased with increasing cycle number, therefore particle agglomeration sintering seems to occur. Sintering reduces the surface area and consequently affects the adsorption [45,46]. The greater slope of the decrease in the conversion diagram suggests the sintering in pristine and hydrated eggshells is higher. This can be confirmed by SEM images taken from used pristine eggshell, hydrated eggshell and sol–gel derived adsorbents and included in Fig. 9. Secondly, the results show that hydration does not have much effect on the CaO conversion, while samples prepared with sol–gel exhibit an

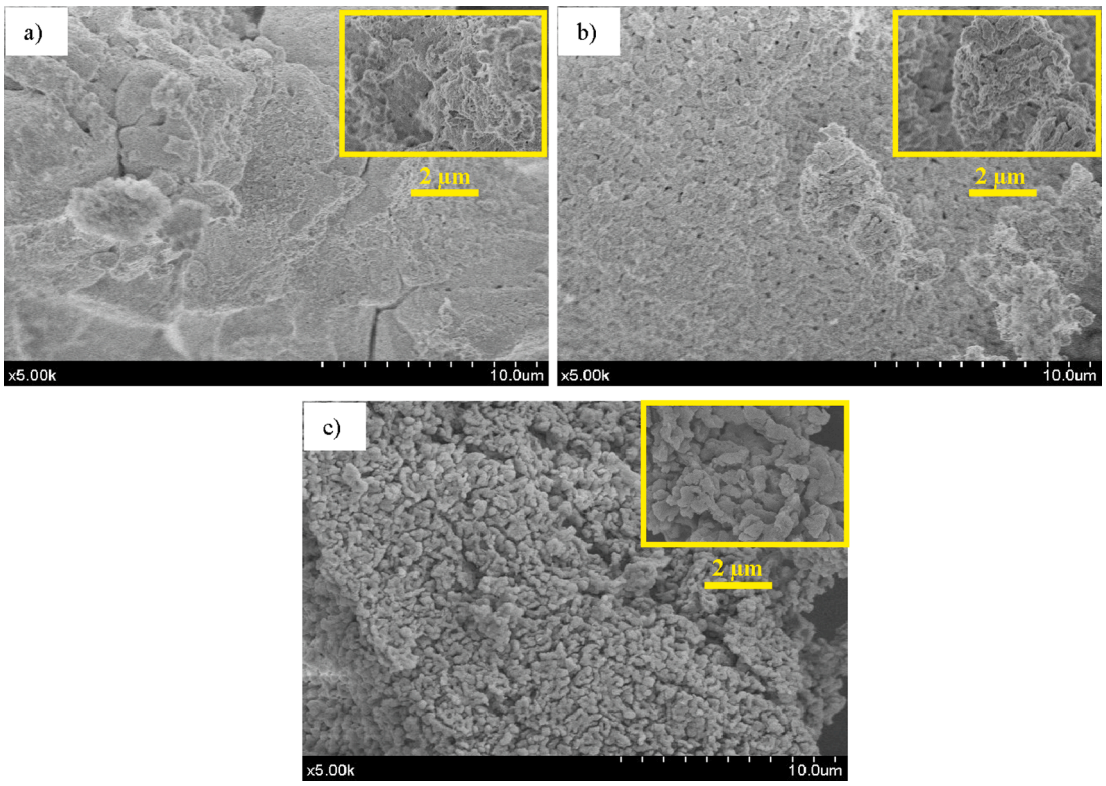

Fig. 9. SEM images of used (a) pristine eggshell (b) hydrated eggshell and (c) sol–gel derived adsorbent after 20th cycle.

improvement in the conversion of about 11.2 and 9.41 % at the end of the 10th and 20th cycles, respectively, most likely because of using HCl in its preparation steps. According to the literature [35], the presence of HCl could significantly change the pore size of calcium-based adsorbents in the CaL process and enhanced their behavior. Arguably, it could be inferred that the chlorine anions on the surface of Ca^{2+} ions avoided the hydroxide ions from the calcium cations owing to the electrostatic repulsive forces created between negatively charged particles [47]. Accordingly, the CaO particles were dispersed more monotonously which led to a diminution of agglomeration. A similar trend also could be concluded from the BET results provided in Table 1 based on which the surface area of sol–gel derived adsorbent was 16.11 and 16.37 % higher than those reported for hydrated and pristine eggshell, respectively. Clearly, hydrated eggshell is not as effective an adsorbent as sol–gel derived adsorbent, thus the latter was elected to further investigation through the addition of silica nanoparticles. In this regard, the effect of adding various weight percentages of silica nanoparticles was investigated only for sol–gel derived adsorbents.

3.2.2. *Effect of silica weight percentages*

In order to ameliorate the agglomeration due to the sintering of sol–gel derived adsorbent, we attempted to modify it by mixing with various weight percentages of silica nanoparticles; including 2.5, 5, 7.5, and 10 wt%. The same procedure was also applied to pristine eggshell particles and the adsorption cycles of CO_2 were compared. Fig. 10 shows the CaO molar conversion obtained, which expresses the amount of CO_2 captured per gram of adsorbent at the beginning of each cycle. Referring to Fig. 10a and b, the sol–gel- derived particles with/without SiO_2 nanoparticles led to higher CO_2 adsorption capacities when compared with their corresponding samples of pristine eggshell particles. For instance, the sol–gel derived adsorbent containing 7.5 % silica nanoparticles still shows 27.59 % higher conversion than pristine eggshell + 7.5 % silica at the end of the 20th cycle. These data were in good agreement with the data reported in Table 1, where the BET surface area of pristine eggshell and sol–gel derived adsorbents containing 7.5 wt% silica nanoparticles were reported as 13.00 and 14.87 m^2/g, respectively. Furthermore, as a surprising result, adding silica nanoparticles up to 7.5 wt% continuously improved the adsorption performance of both pristine eggshell and sol–gel derived adsorbents. However, further increment of the SiO_2 load to 10 wt%, results in reduced CaO conversion in both cases. This phenomenon could be ascribed to the limited sintering that may occur by using of silica nanoparticles at low concentrations. The presence of an appropriate amount of hydrophobic silica nanoparticles may hinder particle agglomeration. This would result in larger effective porosity which facilitates the reaction with CO_2, whereas in the absence of silica nanoparticles.

To sum up, the addition of silica nanoparticles to calcium-based adsorbents helps preserve the surface area and limits the decay in the sorbent's performance. However, using silica nanoparticles with>10 wt % could occupy the adsorbent's active sites and decrease the total capturing capacities.

Considering all the information obtained from the above results, it can be concluded that the most promising percentage of silica in terms of highest CO_2 capturing capacity, was 7.5 wt%. In order to further investigate the role of silica nanoparticles, the relative mass of CO_2 adsorbed and desorbed during the first cycle was extracted from TGA as a function of time. The data for pristine eggshell and sol–gel derived adsorbents with/without 7.5 wt% silica nanoparticles are compared in Fig. 11a and b, respectively. It is well known [48–50] that carbonation reaction occurs in two main stages in the CaL process, the first stage called fast carbonation followed by the second slower carbonation. As shown in Fig. 11, the steep part of the diagram demonstrates the fast carbonation which is limited by surface reaction, while the slower stage characterized by a low slope, is controlled by diffusion. According to Fig. 11a and b, the presence of hydrophobic silica nanoparticles played a role mainly during the fast carbonation and calcination stages, so the relative mass of CO_2 adsorbed in the first cycle of silica-added samples were increased 1.89 and 2.38 times during carbonation process, as compared to the samples without silica. Similarly, the relative mass of CO_2 desorbed in the calcination step had more increment for silica-

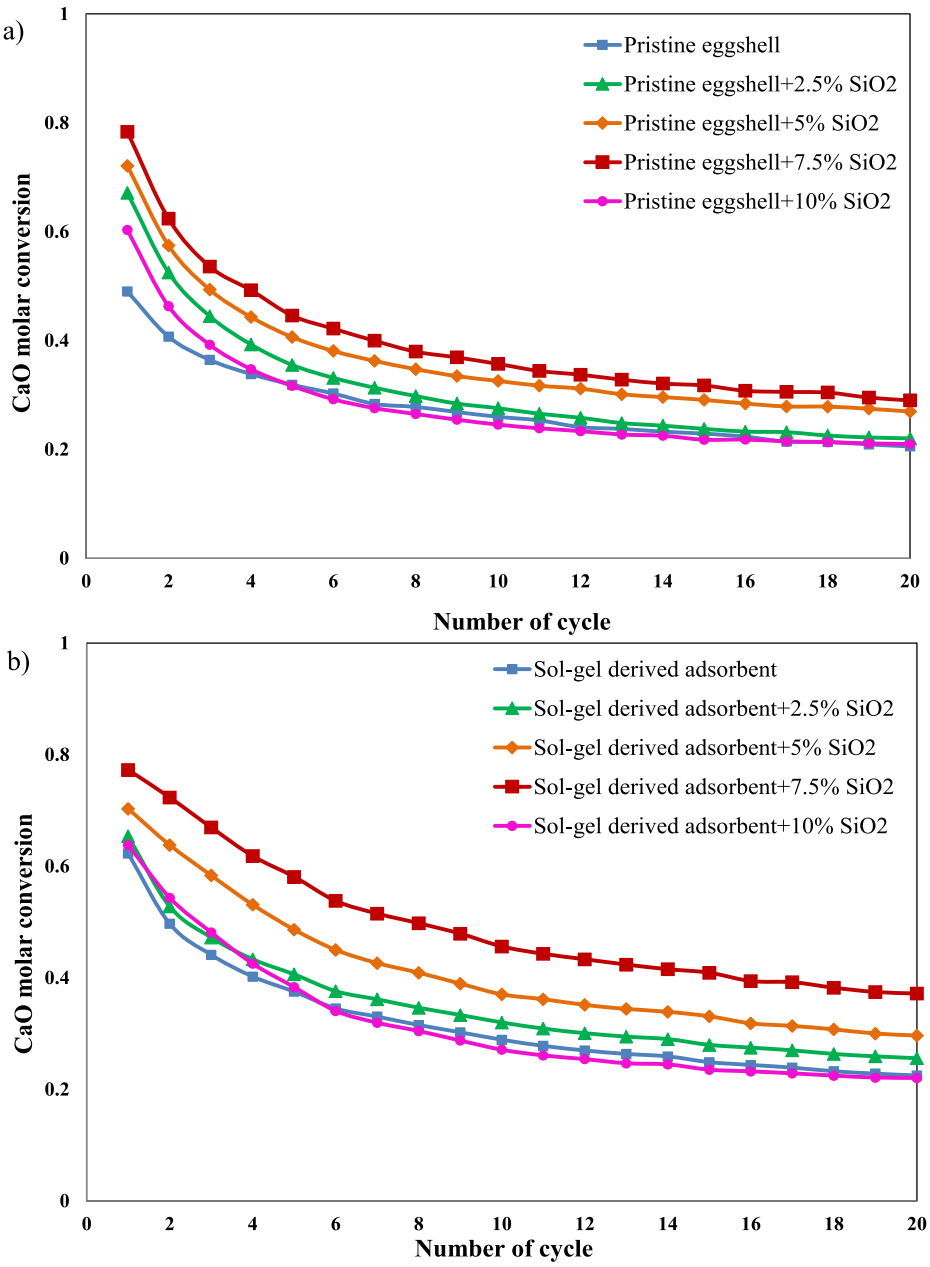

Fig. 10. CaO molar conversion for (a) pristine eggshell and (b) sol–gel derived adsorbent when mixed with different weight percentages of silica nanoparticles.

containing sol–gel derived adsorbent compared to silica-containing pristine eggshell; i. e. 1.41 and 1.17 times, respectively. Interestingly, the relative mass pattern illustrated in Fig. 11, again emphasized the positive effect of synthesizing method even before adding any silica nanoparticles, since, in the absence of silica nanoparticles, the 5.8 % increase in relative mass of CO_2 adsorbed was observed in the fast carbonation stage for the sol–gel derived adsorbent.

Although Fig. 11 demonstrated the positive effect of adding silica nanoparticles in the fast carbonation stage, for accurate investigation of its performance during all 20 cycles, fast carbonation conversion versus cycle number was also shown in Fig. 12, for pristine eggshell and sol–gel derived adsorbent before and after adding 7.5 wt% silica nanoparticles. The same trend as described for the first cycle appeared for all 20 cycles, for instance at the end of the 20th cycle, the fast carbonation conversion of silica-containing pristine eggshell and sol–gel derived adsorbent was increased 2.3 and 2.8 times, compared to the cases without silica. Therefore, not only sol–gel method by itself could slightly increase the fast carbonation conversion for all cycles, but also adding 7.5 wt% silica nanoparticles heightened it more. To sum up, it seemed that the sol–gel method could be an effective procedure to improve the eggshell particles' adsorption performance in the CaL process.

3.3. *Fluidization performance assessment*

As described before, another key parameter in selecting the efficient adsorbent for the CaL process is the adsorbent's fluidizability in a gas–solid fluidized bed system, which cannot be interpreted from the TGA data. The reason may be attributed to the fact that the better gas–solid contact (better fluidizability) leads to a high mass/ heat transfer between gas and particles and then enhances the reaction rate in a fluidized bed. In this regard, investigating the fluidization behavior of the most promising adsorbent selected based on its adsorption behavior; i. e. sol–gel derived adsorbent, in the absence and presence of silica nanoparticles seemed essential. To the best of our knowledge, this type of research has not been reported in the literature. It is also worth mentioning that the real operational CaL process is usually performed in

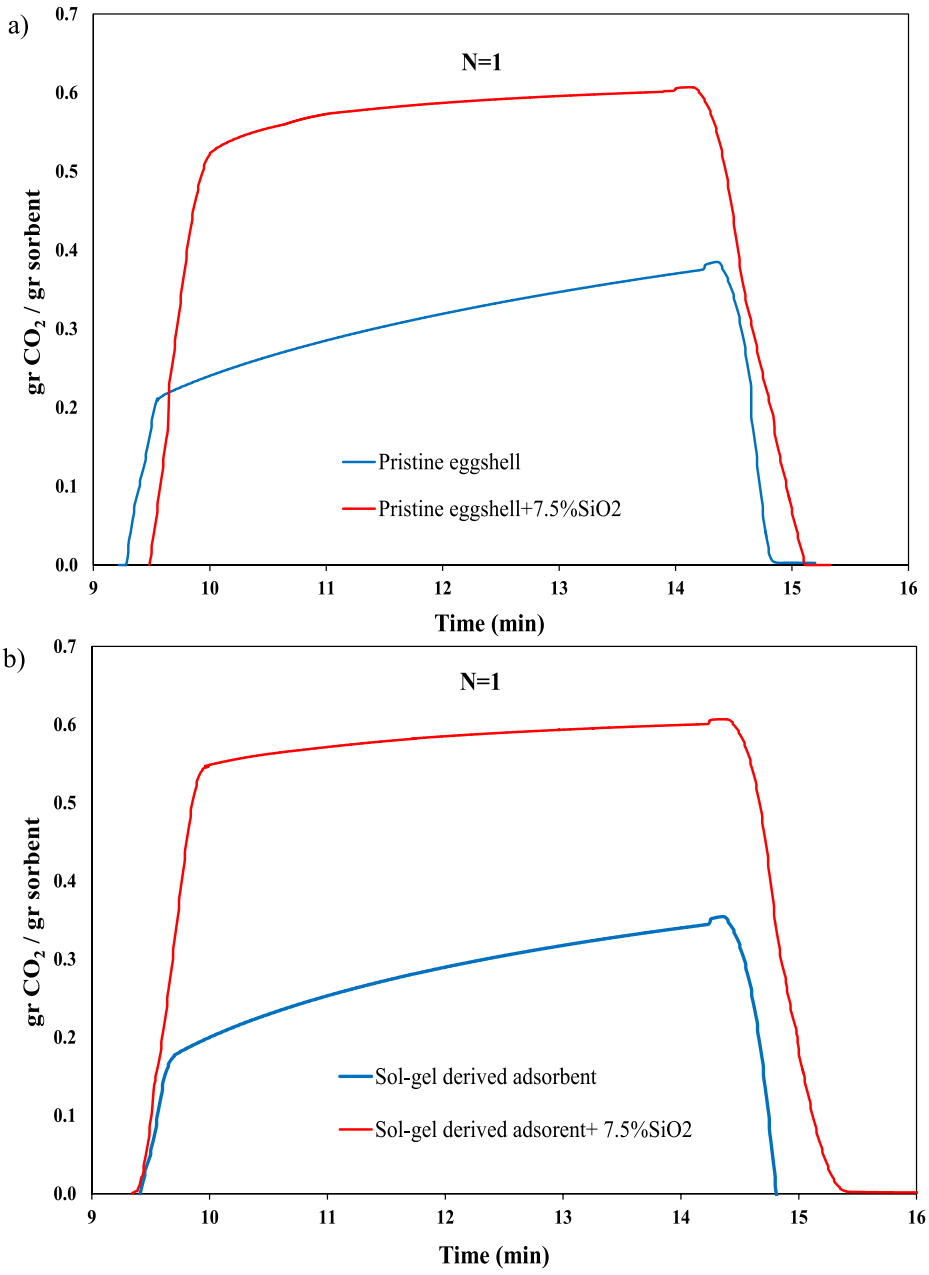

Fig. 11. Relative mass of CO_2 adsorbed and desorbed during the first cycle as a function of time for (a) pristine eggshell and (b) sol–gel derived adsorbent.

the fast fluidization regime, however, it seemed that studying the fluidization behavior of the samples in a lab-scale bed working at low gas velocities of the order of cm/s could be also inspiring. A lab-scale fluidized bed (Fig. 1) at low gas velocities was used in this work to consider the fluidization performance of the adsorbents. For this purpose, both pristine eggshells and also particles synthesized by the sol–gel method were tested in terms of fluidization performance at the gas velocities ranging from 0 to 7 cm/s. Afterward, adding various amounts of hydrophobic silica nanoparticles including 2.5, 5, 7.5, and 10 wt% were performed to study its enhancement effect on the fluidity of samples.

Two main parameters of fluidization assessment including minimum fluidization velocity calculated using the pressure drop variations versus the gas velocity and also bed expansion ratio (H/H_0) were measured for pristine eggshell as well as sol–gel derived adsorbents. The corresponding results were illustrated in Fig. 13. As well documented in the literature [51], the higher bed expansion, and lower minimum fluidization velocity indicate the homogeneity in the particles' fluidity. Fig. 13a showed the digital images of fluidization behavior in terms of bed expansion for pristine eggshell and sol–gel derived adsorbent at a gas velocity of ≈U = 7.31 cm/s. As shown, bed height reached 6.46 cm for sol–gel derived adsorbent which was obviously higher than 5.7 cm, relevant to the pristine eggshell. According to Fig. 13b, although the general trend of the bed expansion graphs was somewhat similar for both pristine eggshell and sol–gel derived particles, varying in the narrow range of 1–1.8, the latter showed a relatively better performance and its bed expansion ratio was 12.5 % higher than that of pristine eggshell, at the gas velocity of ≈6.5 cm/s. This low expansion ratio could be ascribed to the strength of adhesion between fine particles of $CaCO_3$, as a result, the inlet gas couldn't prevail over the adhesion forces. According to later researches [25,52], calcium-based particles were classified as Geldart C with strong cohesive forces that led to the dense agglomerates formation and heterogeneous fluidization behavior. Due to the fast bubbles rising up, no improvement in bed expansion ratio was observed for pristine eggshell particles, when the velocity of inlet gas

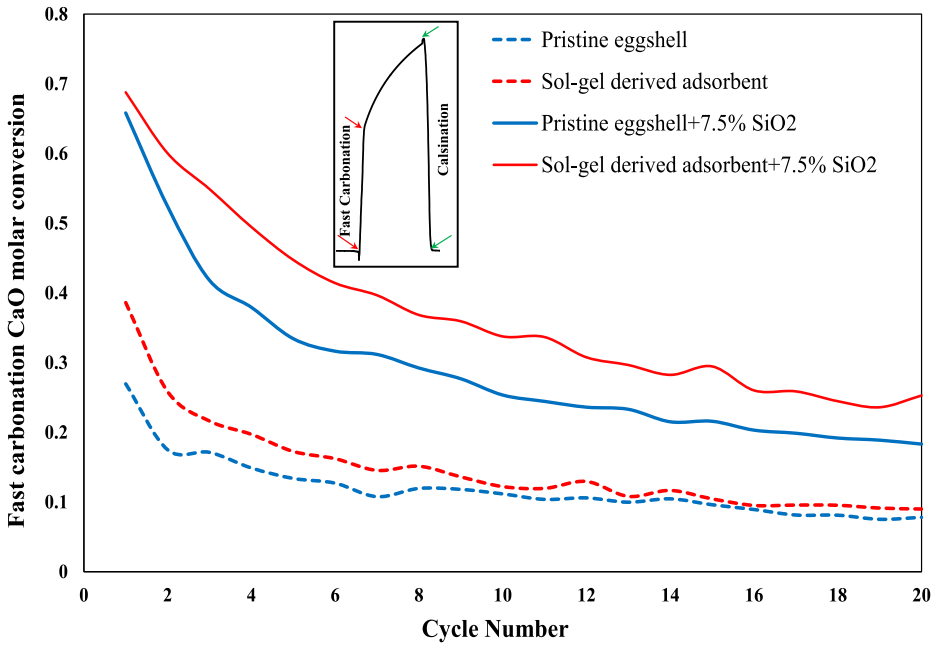

Fig. 12. Fast carbonation conversion for pristine eggshell and sol–gel derived adsorbent during 20 cycles.

was increased>6 cm/s, while the upward trend was rather continued for the sol–gel derived adsorbent. Furthermore, the minimum fluidization velocity in which the pressure drop between both ends of the fluidized bed reached a constant value was obtained as 4.78 cm/s and 4.105 cm/s for the pristine eggshell and sol–gel derived adsorbent, respectively (Fig. 13c), confirming the better performance of the sol–gel derived adsorbent in terms of fluidity.

Since adding specific weight percentages of hydrophobic silica nanoparticles to the sol–gel derived adsorbents enhanced their CO_2 capture capacity, it seemed necessary to investigate the mentioned adsorbents' fluidization performance, as well. As shown in digital images taken from a fluidized bed of sol–gel derived adsorbents containing 10 wt% of silica nanoparticles (Fig. 14a), the altitude increment from 6.46 cm to 9.2 cm affirmed the positive role of silica nanoparticles on the fluidity of sol–gel derived adsorbents, hereupon the sever channels were replaced by agglomerate particulate fluidization (APF) behavior and as a result liquid- like fluidization was appeared. In fact, covering the $CaCO_3$ particles synthesized with the sol–gel method with easily fluidizable hydrophobic silica nanoparticles, reduced the inter-particle forces and prevented them from the formation of the large agglomerates [53]. Fig. 14b showed the bed expansion ratio for sol–gel derived adsorbents in presence of silica nanoparticles at different gas velocities in the range of 0–7.5 cm/s. As seen, adding even a very low amount of silica nanoparticles (2.5 wt%) affected the bed expansion ratio. It was evident that by increasing the silica nanoparticles' weight percentage from 2.5 to 10 %, the bed expansion ratio was also extended, especially at high gas velocities. In more detail, the bed expansion ratio for adsorbent + 2.5, 5, 7.5, and 10 wt% of silica nanoparticles at the gas velocity of ≈6.5 cm/s reached 1.86, 2.11, 2.29, and 2.52, respectively. In order to determine the minimum fluidization velocity for all silica-added samples, the pressure drop changes with superficial gas velocity were plotted in Fig. 14c. It could be observed that by increasing the silica nanoparticles proportion in the base adsorbent, the minimum fluidization velocity was decreased so that its value was equal to 4.329, 4.098, 3.89, and 3.14 for 2.5, 5, 7.5, and 10 wt% silica-added samples, respectively. The better fluidization performance achieved with a higher amount of silica nanoparticles could be ascribed to the contact charging and electrostatic attraction forces developed at the surface contact points between the eggshell-derived particles and silica nanoparticles [15].

Although it seemed that increasing the weight percentage of silica nanoparticles had a beneficial effect on the fluidization behavior of adsorbents, there should be some limits on SiO_2 content. Since silica nanoparticles are not a CO_2 adsorbent, using an excessive amount could adversely affect the capturing capacity of eggshell-derived particles by decreasing the CaO fraction available for carbonation. Meanwhile, in lower weight percentages of silica nanoparticles, the contribution of CO_2 diffused into the adsorbent particles was improved, because of adhesion diminution between the eggshell particles. Therefore, according to the adsorption results obtained by using various silica nanoparticles weight percentages; 7.5 wt% of this additive played a better role while adding 10 wt% of silica nanoparticles decreased the CaO conversion. By the end, it seemed that the sol–gel derived adsorbent containing 7.5 wt% silica nanoparticles could be introduced as the most promising adsorbent due to the simultaneous improvement in adsorption and fluidization performance. It is worth mentioning that, many researchers have analyzed numerous calcium-based adsorbents by using TGA, however, the industrial CO_2 removal process carries out in a fluidized bed in which a uniform fluidization behavior of CO_2 adsorbents is a fundamental requirement. Results reported here confirmed the superior potential in fluidized bed systems of eggshell particles as a base material for synthesizing of sol–gel derived adsorbent modified with 7.5 wt% of silica nanoparticles. In summarizing, the development of a novel, green, readily scalable, cost-effective calcium-based adsorbent derived from the eggshell and SiO_2 NPs leads to a new composite with enhanced homogeneous fluidity and capturing capacity compared to other chemicals, in the cyclic CO_2 removing process. Heidari et al [23] applied different weight percentages of hydrophobic silica nanoparticles to sol–gel derived composites including Ca/Zr/Al/Ce, Ca/Al/Ce and Ca/Al as CO_2 adsorbents where in the presence of 10 wt% SiO_2, the bed expansions were about 2.4, 2.2 and 2.15, respectively in the gas velocity of 5 cm/s. Similarly, Azimi et al [20] investigated the fluidity of Al-based synthesized CaO sorbents prepared by sol–gel method using calcium nitrate and aluminum nitrate as precursors for which the bed expansion ratio of 2.4 was reached while mixing with 10 wt% silica nanoparticles. The sol–gel derived adsorbent introduced in this work at the same amount of silica nanoparticles (10 wt%) showed the bed expansion of about 2.5. Furthermore, the molar conversion of the most promising adsorbent (sol–gel derived adsorbent + 7.5 wt% silica) could be compared with other materials such as limestone or dolomite. Juan Miranda-Pizarro et al [6] reported values of 0.04 and 0.1 for CaO

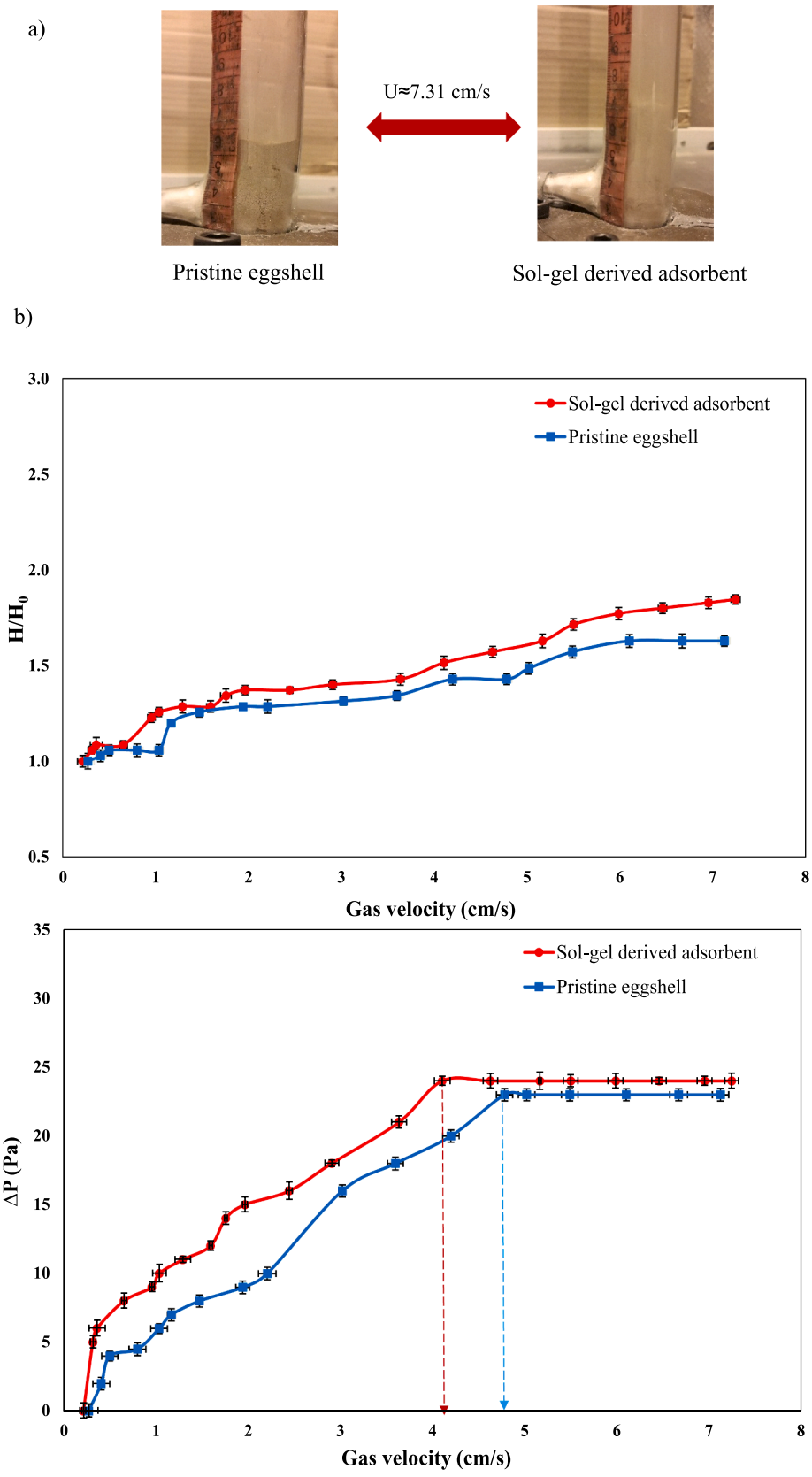

Fig. 13. (a) Digital images for fluidization behavior of pristine eggshell (left figure) and sol–gel derived adsorbent (right figure) at U≈7.31 cm/s, along with their (b) bed expansion and (c) pressure drop curves.

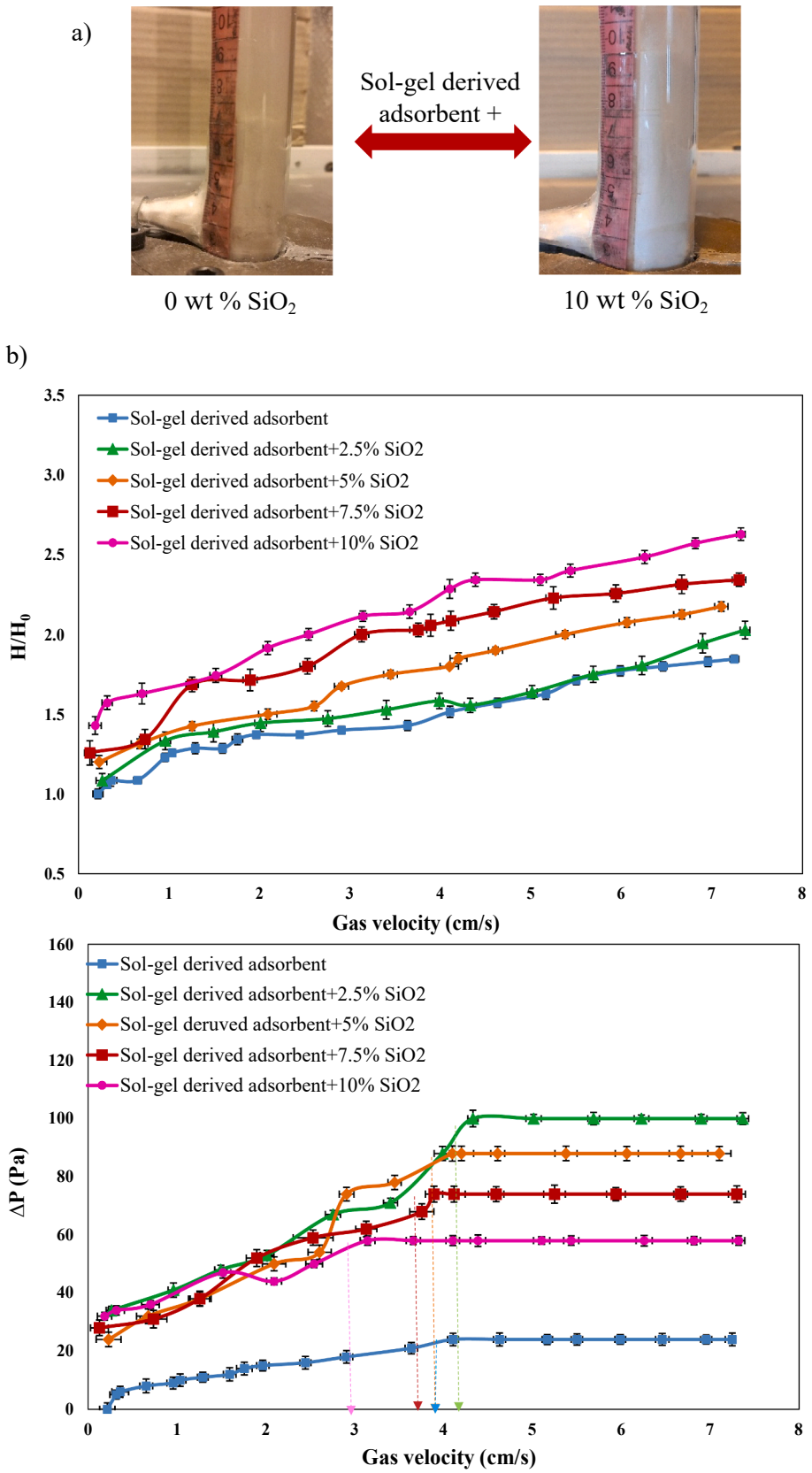

Fig. 14. (a) Digital images for fluidization behavior of sol–gel derived adsorbents before (left figure) and after adding 10 wt% silica NPs (right figure) at U≈7.31 cm/s, along with their (b) bed expansion and (b) pressure drop curves in the presence of different weight percentages of silica NPs.

conversion in fast reaction controlled phase for limestone and dolomite at the end of 20th cycle, while the corresponding amount for selected adsorbent here was 0.26 (Fig. 12). This adsorbent also showed doubled total molar conversion compared to pure CaO particles presented at [23], at the end of 20th cycle.

Finally, it can be stated that in spite of the favorable results reported in the current manuscript for operational applications, further necessary steps should be considered to solve the remaining challenges in forthcoming studies. For instance, using a real high-temperature fluidized bed for fluidization assessment and also performing carbonation/calcination cycles in an industrially scaled fluidized bed reactor instead of TGA is recommended. The elutriation and attrition of particles in fluidized beds performing under realistic streams should be also addressed as a challenging issue. Another important issue in the discussion of fluidity of fine particles on an industrial scale is elutriation. Improving the mechanical strength of adsorbents is required to alleviate their elutriation in realistic fluidized-bed reactors. The granulation of solid adsorbents through various techniques, including extrusion-spheronization [54], extrusion [55] and rotation [56] have been proposed to boost the mechanical strength and anti-attrition of solid adsorbents.

4. Conclusions

In this study, we developed novel, green and cost-effective SiO_2-decorated calcium-based adsorbents derived from eggshell waste by two different preparation methods of hydration and sol–gel to capture the CO_2 greenhouse gas. The capability of prepared adsorbents to be used in the CaL process was investigated through two main objectives i.e., CO_2 capture capacity and fluidization performance. In this regard, the sol–gel derived adsorbents were selected as the most promising sample based on the TGA results. Modification of the adsorbents was exerted by adding several weight percentages of hydrophobic silica nanoparticles to the sol–gel derived adsorbents as well as the pristine eggshell for comparison. The highest CaO conversion was reported for sol–gel derived adsorbent with 7.5 wt% of silica nanoparticles which was 27.59 % higher than the corresponding amount for pristine eggshell contained 7.5 % silica nanoparticles after 20th cycles. Pursuing the second aim of this research, the fluidizability of the sol–gel derived adsorbents in the presence of various amounts of silica nanoparticles was studied using a lab-scale fluidized bed at the gas velocity ranges from 0 to 7.5 cm/s. The results confirmed the positive effect of adding silica nanoparticles even in very small amounts; the higher silica nanoparticles led to higher bed expansion and lower minimum fluidization velocity. The corresponding values for bed expansion ratio at U≈7.31 cm/s, and minimum fluidization velocity of sol–gel derived adsorbent containing 10 wt% silica nanoparticles, was reported as 42 % increment and 14 % decrement compared to the silica-free sol–gel derived adsorbent, respectively. Therefore, it could be seen that using silica nanoparticles could transform the heterogeneous fluidization behavior to agglomerate particulate fluidization. Since 10 wt% of silica NPs decreased the CaO conversion of both pristine eggshells and the sol–gel derived adsorbents over 20 cycles, it seemed logical to introduce 7.5 wt% silica nanoparticles as the effective amount of this additive in terms of both capture capacity and fluidization performance.

Funding

This work was supported by University of Tabriz, International and Academic Cooperation Directorate, in the framework of TabrizU-300 program.

CRediT authorship contribution statement

Mehri Imani: Investigation, Methodology, Writing – original draft. **Maryam Tahmasebpoor:** Supervision. **Pedro Enrique Sánchez-Jiménez:** Investigation, Validation. **Jose Manuel Valverde:** Investigation. **Virginia Moreno:** Investigation.

Declaration of Competing Interest

The authors declare that they have no known competing financial interests or personal relationships that could have appeared to influence the work reported in this paper.

Data availability

The authors do not have permission to share data.

References

[1] S.T. Bararpour, D. Karimi, N. Mahinpey, Investigation of the effect of alumina-aerogel support on the CO_2 capture performance of K_2CO_3, Fuel 242 (2019) 124–132, https://doi.org/10.1016/J.FUEL.2018.12.123.
[2] O. Edenhofer, Mitigation of climate change: contribution of working group III to the fifth assessment report of the intergovernmental panel on climate change, Cambridge University Press, 2014, pp. 413–510.
[3] M. Erans, V. Manovic, E.J. Anthony, Calcium looping sorbents for CO_2 capture, Appl. Energy 180 (2016) 722–742, https://doi.org/10.1016/j.apenergy.2016.07.074.
[4] J.M. Valverde, P.E.S. Jimenez, L.A.P. Maqueda, High and stable CO_2 capture capacity of natural limestone at Ca-looping conditions by heat pretreatment and recarbonation synergy, Fuel 123 (2014) 79–85, https://doi.org/10.1016/j.fuel.2014.01.045.
[5] J. Blamey, E.J. Anyhony, J. Wang, J.P.S. Fennell, The calcium looping cycle for large-scale CO_2 capture, Prog. Energy Combust. Sci. 36 (2010) 260–279, https://doi.org/10.1016/j.pecs.2009.10.001.
[6] J.M. Pizarro, A. Perejon, J.M. Valverde, L.A.P. Maqueda, P.E.S. Jiménez, CO_2 capture performance of Ca-Mg acetates at realistic calcium looping conditions, Fuel. 196 (2017) 497–507, https://doi.org/10.1016/j.fuel.2017.01.119.
[7] A. Mavropoulos, C.W. David, J. Cooper, C. Vells, B. Appelqvist, Globalization and waste management, International Solid Waste association, 2012, pp. 1–55.
[8] R. Sun, R. Xiao, J. Ye, Kinetic analysis about the CO_2 capture capacity of lime mud from paper mill in calcium looping process, Energy Sci. Eng. 8 (2020) 4014–4024, https://doi.org/10.1002/ese3.792.
[9] J.M. Pizarro, A. Perejon, J.M. Valverde, P.E.S. Jiménez, L.A.P. Maqueda, On the use of steel slag for CO_2 capture at realistic calcium looping conditions, RSC Advances 6 (2016) 37656–37663, https://doi.org/10.1039/C6RA03210A.
[10] X. Ma, Y. Li, C. Chi, W. Zhang, J. Shi, L. Duan, CO_2 Capture Performance of mesoporous synthetic sorbent fabricated using carbide slag under realistic calcium looping conditions, Energy Fuels 31 (2017) 7299–7308, https://doi.org/10.1021/acs.energyfuels.7b00676.
[11] S. Castilho, A. Kiennemann, M. Francisco, C. Pereira, P.S. Dias, Sorbents for CO_2 capture from biogenesis calcium wastes, Chem. Eng. J. 226 (2013) 146–153, https://doi.org/10.1016/j.cej.2013.04.017.
[12] E.R. Sacia, S. Ramkumar, N. Phalak, L.S. Fan, Synthesis and regeneration of sustainable CaO sorbents from chicken eggshells for enhanced carbon dioxide capture, ACS Sustainable Chemical Engineering 1 (2013) 903–909, https://doi.org/10.1021/sc300150k.
[13] J.J.A. Troya, P.E.S. Jimenez, A. Perejón, J.M. Valverde, R. Chacartegui, L.A. P. Maqueda, Calcium-looping performance of biomineralized $CaCO_3$ for CO_2 capture and thermochemical energy storage, Ind. Eng. Chem. Res. 59 (2020) 12924–12933, https://doi.org/10.1021/acs.iecr.9b05997.
[14] H.R. Radfarnia, M.C. Iliuta, Metal oxide-stabilized calcium oxide CO_2 sorbent for multicycle operation, Chem. Eng. J. 232 (2013) 280–289, https://doi.org/10.1016/j.cej.2013.07.049.
[15] M.J. Nobarzad, M. Tahmasebpoor, M. Imani, C. Pevida, S.Z. Heris, Improved CO2 adsorption capacity and fluidization behavior of silica-coated amine-functionalized multi-walled carbon nanotubes, J. Environ. Chem. Eng. 9 (2021), 105786, https://doi.org/10.1016/j.jece.2021.105786.
[16] J.M. Valverde, P.E.S. Jimenez, L.A.P. Maqueda, Role of precalcination and regeneration conditions on postcombustion CO_2 capture in the Ca-looping technology, Appl. Energy 136 (2014) 347–356, https://doi.org/10.1016/j.apenergy.2014.09.052.
[17] R.H. Borgwardt, Sintering of nascent calcium oxide, Chem. Eng. Sci. 44 (1989) 53–60, https://doi.org/10.1016/0009-2509(89)85232-7.
[18] M. Heidari, M. Tahmasebpoor, S.B. Mousavi, C. Pevida, CO_2 capture activity of a novel CaO adsorbent stabilized with (ZrO_2+ Al_2O_3+ CeO_2)-based additive under mild and realistic calcium looping conditions, Journal of CO_2 Utilization 53 (2021), 101747, https://doi.org/10.1016/j.jcou.2021.101747.
[19] J.Y. Jing, T.Y. Li, X.W. Zhang, S.D. Wang, J. Feng, W.A. Turmel, W.Y. Li, Enhanced CO_2 sorption performance of CaO/$Ca_3Al_2O_6$ sorbents and its sintering-resistance mechanism, Appl. Energy 199 (2017) 225–233, https://doi.org/10.1016/j.apenergy.2017.03.131.
[20] B. Azimi, M. Tahmasebpoor, P.E.S. Jimenez, A. Perejon, J.M. Valverde, Multicycle CO_2 capture activity and fluidizability of Al-based synthesized CaO sorbents, Chem. Eng. J. 358 (2019) 679–690, https://doi.org/10.1016/j.cej.2018.10.061.

[21] R. Koirala, G.K. Reddy, P.G. Smirniotis, Single nozzle flame-made highly durable metal doped Ca-based sorbents for CO_2 capture at high temperature, Energy Fuels 26 (2012) 3103–3109, https://doi.org/10.1021/ef3004015.

[22] Y. Li, C. Zhao, H. Chen, L. Duan, X. Chen, Cyclic CO_2 capture behavior of $KMnO_4$-doped CaO-based sorbent, Fuel 89 (2010) 642–649, https://doi.org/10.1016/j.fuel.2009.08.041.

[23] M. Heidari, M. Tahmasebpoor, A. Antzara, A.A. Lemonidou, CO_2 capture and fluidity performance of CaO-based sorbents: Effect of Zr, Al and Ce additives in tri-, bi- and mono-metallic configurations, Process Saf. Environ. Prot. 144 (2020) 349–365, https://doi.org/10.1016/j.psep.2020.07.041.

[24] J.M. Valverde, F. Pontiga, C.S. Hoyo, M.A. Quintanilla, H. Moreno, F.J. Duran, M. J. Espin, Improving the gas–solids contact efficiency in a fluidized bed of CO_2 adsorbent fine particles, PCCP 13 (2011) 14906–14909, https://doi.org/10.1039/C1CP21939A.

[25] O. Amjadi, M. Tahmasebpoor, H. Aghdasinia, Fluidization behavior of cohesive Ca $(OH)_2$ powders mixed with hydrophobic silica nanoparticles, Chemical, Eng. Technol. 42 (2019) 287–296, https://doi.org/10.1002/ceat.201800007.

[26] M. Imani, M. Tahmasebpoor, P.E.S. Jimenez, J.M. Valverde, V. Moreno, Improvement in cyclic CO_2 capture performance and fluidization behavior of eggshell-derived $CaCO_3$ particles modified with acetic acid used in calcium looping process, CO_2 Utilization 65 (2022), 102207, https://doi.org/10.1016/j.jcou.2022.102207.

[27] Z. Skoufa, A. Antezara, E. Heracleousb, A.A. Lemonidou, Evaluating the activity and stability of CaO-based sorbents for postcombustion CO_2 capture in fixed-bed reactor experiments, Energy Procedia 86 (2016) 171–180, https://doi.org/10.1016/j.egypro.2016.01.018.

[28] K. Wang, P. Zhao, X. Guo, D. Han, Y. Chao, High-temperature CO_2 capture cycles of hydrated limestone prepared with aluminum (hydr)oxides derived from kaolin, Energy Convers. Manage. 86 (2014) 1147–1153, https://doi.org/10.1016/j.enconman.2014.06.092.

[29] B. Yoosuk, P. Udomsap, B. Puttasawat, P. Krasae, Modification of calcite by hydration–dehydration method for heterogeneous biodiesel production process: The effects of water on properties and activity, Chem. Eng. J. 162 (2010) 135–141, https://doi.org/10.1016/j.cej.2010.05.013.

[30] L. Habte, N. Shiferaw, D. Mulatu, T. Thenepalli, R. Chilakala, J.W. Ahn, Synthesis of nano-calcium oxide from waste eggshell by Sol-Gel method, Sustainability 11 (2019) 3196, https://doi.org/10.3390/su11113196.

[31] H. Klug, L. Alexander, X-ray Diffraction Procedures, John Wiley and SonsInc, New York, 1962.

[32] C. Sun, X. Yan, Y. Li, J. Zhao, Z. Wang, Coupled CO_2 capture and thermochemical heat storage of CaO derived from calcium acetate, Greenhouse Gas Science Technology 10 (2020) 1027–1038, https://doi.org/10.1002/ghg.2021.

[33] L.Q. Carballo, M.d.R.P. Perez, D.C. Fernández, A.C. Amores, J.M.F. Rodríguez, Optimum particle size of treated calcites for CO_2 capture in a power plant, Paterials 12 (2019) 1284, https://doi.org/10.3390/ma12081284.

[34] J.D.D. Martín, P.E.S. Jemenez, J.M. Valverde, A. Perejón, J.A. Troya, P.G. Trinanes, L.A.P. Maqueda, Role of particle size on the multicycle calcium looping activity of limestone for thermochemical energy storage, J. Adv. Res. 22 (2020) 67–76, https://doi.org/10.1016/j.jare.2019.10.008.

[35] M.J.A. Jeboori, M. Nguyen, C. Dean, P.S. Fennell, Improvement of limestone-based CO_2 sorbents for Ca looping by HBr and Other mineral acids, Ind. Eng. Chem. Res. (2012) 1426–1433, https://doi.org/10.1021/ie302198g.

[36] M.A.S. Quintanilla, J.M. Valverde, M.J. Espin, A. Castellanos, Electrofluidization of silica nanoparticle agglomerates, Ind. Eng. Chem. Res. 51 (2011) 531–538, https://doi.org/10.1021/ie200538v.

[37] J.M. Valverde, M. Quintanilla, M.J. Espin, A. Castellanos, Nanofluidization electrostatics, Phys. Rev. 77 (2008), 031301, https://doi.org/10.1103/PhysRevE.77.031301.

[38] A.N. Shafawi, A.R. Mohamed, P. Lahijani, M. Mohammadi, Recent advances in developing engineered biochar for CO_2 capture: An insight into the biochar modification approaches, J. Environ. Chem. Eng. 9 (2021), 106869, https://doi.org/10.1016/j.jece.2021.106869.

[39] M. Waqas, Z. Asam, M. Rehan, M.N. Anwar, R.A. Khattak, I.M.I. Ismail, M. Tabatabaei, A.S. Nizami, Development of biomass-derived biochar for agronomic and environmental remediation applications, Biomass Convers. Biorefin. 11 (2020) 339–361, https://doi.org/10.1007/s13399-020-00936-2.

[40] J.M. Valverde, A. Perejon, L.A.P. Maqueda, Enhancement of Fast CO_2 Capture by a Nano-SiO_2/CaO Composite at Ca-Looping Conditions, Environ. Sci. Technol. 46 (2012) 6401–6408, https://doi.org/10.1021/es3002426.

[41] J.M. Valverde, F. Pontiga, C.S. Hoyo, M.A.S. Quintanilla, H. Moreno, F.J. Duran, M. J. Espin, Improving the gas solids contact efficiency in a fluidized bed of CO_2 adsorbent fine particles, PCCP 13 (2011) 14906–14909, https://doi.org/10.1039/C1CP21939A.

[42] A.W. Adamson, Physical Chemistry of Surfaces, Fifth edittion (1990), New York, John Wiley and Sons. ISBN 0-471-61019-4.

[43] N.A. Seaton, Determination of the connectivity of porous solids from nitrogen sorption measurements, Chem. Eng. Sci 46 (1991) 1895–1909, https://doi.org/10.1016/0009-2509(91)80151-N.

[44] F. Yan, J. Jiang, X. Chen, S. Tian, K. Li, Synthesis and characterization of silica nanoparticles preparing by low-temperature vapor-phase hydrolysis of $SiCl_4$, Ind. Eng. Chem. Res. 53 (2014) 11884–11890, https://doi.org/10.1021/ie501759w.

[45] M. Tahmasebpoor, L.D. Martin, M. Talebi , N. Mostoufi, J.R.V. Ommen, Fluidization of nanoparticles: the effect of surface characteristics, in The 14th International Conference On Fluidization From fundamentals To Products (2013), Netherlands, http://dc.engconfintl.org/fluidization_xiv.

[46] M. Tahmasebpoor, R.G.S. Abadi, Y.R. Noupoor, P. Badamchizadeh, A Model based on electrostatic repulsion and hydrogen bond forces to estimate the size of nanoparticle agglomerates in fluidization, Ind. Eng. Chem. Res. 55 (2016) 12939–12948, https://doi.org/10.1021/acs.iecr.6b02792.

[47] S.L. Hsieh, F.Y. Li, P.Y. Lin, D.E. Beck, R. Kirankumar, G.J. Wang, S. Hsieh, CaO recovered from eggshell waste as a potential adsorbent for greenhouse gas CO_2, J. Environ. Manage. 297 (2021), 113430, https://doi.org/10.1016/j.jenvman.2021.113430.

[48] B. Arias, J.C.A. Grasa, G.S.G. Adiego, An analysis of the effect of carbonation conditions on CaO deactivation curves, Chem. Eng. J. 167 (2011) 255–261, https://doi.org/10.1016/j.cej.2010.12.052.

[49] S.K. Bathia, D.D. Perlmutter, Effect of the product layer on the kinetics of the CO_2-lime reaction, AIChE J. 19 (1983) 79–86, https://doi.org/10.1002/aic.690290111.

[50] F. Sattari, M. Tahmasebpoor, J.M. Valverdeb, C. Ortizc, M. Mohammadpourfard, Modelling of a fluidized bed carbonator reactor for post-combustion CO_2 capture considering bed hydrodynamics and sorbent characteristics, Chem. Eng. J. 406 (2021), 126762, https://doi.org/10.1016/j.cej.2020.126762.

[51] M.J. Nobarzad, M. Tahmasebpoor, M. Heidari, C. Pevida, Theoretical and experimental study on the fluidity performance of hard-to-fluidize carbon nanotubes-based CO_2 capture sorbents, Front. Chem. Sci. Eng. (2022) 1–16, https://doi.org/10.1007/s11705-022-2159-x.

[52] O. Amjadi, M. Tahmasebpoor, Parametric investigation: Improving fluidization behavior of cohesive $Ca(OH)_2$ adsorbent using hydrophilic silica nanoparticles, Particuology 40 (2018) 52–61, https://doi.org/10.1016/j.partic.2017.12.004.

[53] M. Tahmasebpoor, Y.R. Noupoor, P. Badamchizadeh, Fluidity enhancement of hard-to-fluidize nanoparticles by mixing with hydrophilic nanosilica and fluid catalytic cracking particles: Experimental and theoretical study, Phys. Fluids 31 (2019), 073301, https://doi.org/10.1063/1.5100064.

[54] J. Sun, W. Liu, Y. Hu, J. Wu, M. Li, X. Yang, W. Wang, M. Xu, Enhanced performance of extruded–spheronized carbide slag pellets for high temperature CO_2 capture, Chem. Eng. J. 285 (2016) 293–303, https://doi.org/10.1016/j.cej.2015.10.026.

[55] C. Qin, J. Yin, H. An, W. Liu, B. Feng, Performance of extruded particles from calcium hydroxide and cement for CO_2 capture, Energy Fuels 26 (2012) 154–161, https://doi.org/10.1021/ef201141z.

[56] V. Manovic, Y. Wu, I. He, E.J. Anthony, Spray water reactivation/pelletizationof spent CaO-based sorbent from calcium looping cycles, Environtal Science Technology 46 (2012) 12720–12725, https://doi.org/10.1021/es303252j.